Int. J. Multiphase Flow Vol. 14, No. 5, pp. 587–606, 1988
Printed in Great Britain.

0301-9322/88 $3.00 + 0.00

THE EFFECTS OF BUBBLES ON THE VOLUME FLUXES AND THE PRESSURE GRADIENTS IN UNSTEADY AND NON-UNIFORM FLOW OF LIQUIDS

R. KOWE,[1] J. C. R. HUNT,[1]† A. HUNT,[2] B. COUET[2]
and L. J. S. BRADBURY[3]

[1]Department of Applied Mathematics and Theoretical Physics, University of Cambridge, Silver Street, Cambridge, Cambs., England

[2]Schlumberger Cambridge Research, Madingley Road, Cambridge, Cambs., England

[3]Department of Mechanical Engineering, Plymouth Polytechnic, Drake Circus, Plymouth, Devon, England

(*Received* 13 *May* 1987; *in revised form* 18 *April* 1988)

Abstract—In this paper the motion of a single bubble or particle in an accelerating liquid flow is analysed using a generalized force equation. The motion of the bubble relative to the fluid gives rise to a drift flux of liquid which affects the mean flow field of the liquid. This flux is calculated in terms of the effective or added mass coefficient of the bubble, C_m, which is equal to 1/2 for a small bubble at high Reynolds number. By analysis of the flow in terms of the three flow fields associated with the interstitial liquid, the displaced liquid and the bubble itself, we obtain a rational method for calculating the forces acting on the bubble, the mass conservation equations and the pressure field in the liquid. For a bubbly flow with low void fraction this form of the mass conservation equation reduces to an expression for liquid and gas superficial velocity as a function of relative velocity (the slip measured relative to the interstitial velocity, to be defined) and void fraction, where the constants are defined in terms of C_m. Unlike the commonly used relation of Zuber & Findlay (1965), our expression can be generalized to non-uniform flows. Our predictions (using $C_m = 1/2$) agree with Zuber & Findlays' empirical equations for low void fraction ϵ in a vertical pipe. They do not, however, agree for high values of ϵ. A new analysis of the mean pressure field in disperse two-phase flow is presented. While the bubbles respond to the interstitial velocity and pressure field, the pressure of interest is usually the average over the *whole* liquid volume. We show how these are related. The models developed here are applied to the practically important flow of air bubbles in an inclined nozzle, and are compared with recent laboratory measurements.

Key Words: bubbly flows, accelerating flows, multiphase pipe flows

1. INTRODUCTION

Recent research has led to a better understanding of the forces on bubbles and particles in non-uniform unsteady flows. In particular, earlier misunderstandings about the form of added mass forces were clarified.

The first problem has been to generalize the classical result for the force $\mathbf{F}_I$ on a sphere moving with velocity $\mathbf{v}$ in a uniform steady flow $\mathbf{u}_0(t)$ of an inviscid fluid,

$$\mathbf{F}_I = \rho_L V_b \left[(1 + C_m) \frac{\mathrm{d}\mathbf{u}_0}{\mathrm{d}t} - C_m \frac{\mathrm{d}\mathbf{v}}{\mathrm{d}t} \right], \qquad [1]$$

to a non-uniform unsteady flow. By analysing inviscid flow around a sphere in rotational straining flow, Thomas *et al.* (1983) and Auton *et al.* (1987; Auton 1987) concluded that the interfacial force on a sphere that is small compared with the length over which the velocity gradients vary is

$$F_{Ii} = \rho_L V_b \left\{ (1 + C_m) \frac{\mathrm{D}u_{0i}}{\mathrm{D}t} - C_m \frac{\mathrm{d}v_i}{\mathrm{d}t} - g_i - [C_L(\mathbf{v} - \mathbf{u}_0) \times \boldsymbol{\omega}]_i \right\}. \qquad [2a]$$

Here $\mathbf{u}$ and $\boldsymbol{\omega}$ are the liquid velocity and vorticity ($\boldsymbol{\omega} = \nabla \times \mathbf{u}_0$) in the absence of the bubble and $\mathrm{D}u_{0i}/\mathrm{D}t$ is the liquid acceleration at the location ($\mathbf{x}_b$) of the bubble and is defined by

$$\frac{\mathrm{D}u_{0i}}{\mathrm{D}t} = \left(\frac{\partial u_{0i}}{\partial t} + u_{0j} \frac{\partial u_{0i}}{\partial x_j} \right) \qquad (\mathbf{x} = \mathbf{x}_b), \qquad [2b]$$

†To whom all correspondence should be addressed.

where ρ_L and ρ_G are the liquid and gas densities, V_b is the volume of the bubble, g_i is the acceleration due to gravity [$=(-g, 0, 0)$, if x is vertical] and C_L is the bubble lift coefficient. Expression [2a] has been derived by a number of authors for *irrotational* flow, these are reviewed by Thomas *et al.* (1983).

We shall follow the suggestion of Thomas *et al.* (1983) that a viscous drag $\mathbf{F}_D$ can be simply added to the inviscid force, so that the total interfacial force on a spherical bubble is

$$F_i = F_{Ii} + F_{Di}, \qquad [3a]$$

where F_{D_i} can be conveniently defined in terms of V_t the terminal rise (or fall) speed of the bubble in stationary liquid (at the same Reynolds number):

$$F_{Di} = -\rho_L V_b \frac{|\Delta\rho|}{\rho_L} g \frac{(v_i - u_{0i})}{V_t} f\left(\frac{v_i - u_{0i}}{V_t}\right), \qquad [3b]$$

where $\Delta\rho = \rho_G - \rho_L$. Usually, V_t is better known than the drag coefficient C_D or the bubble radius a. For a spherical bubble in a pure liquid $f = 1$, and for a high Reynolds number bubble in dirty liquid, where C_D is approximately constant, $f = |v_i - u_{0i}|/V_t$ (see appendix A).

We ignore the effects of the wakes and the turbulence produced by bubbles (of importance in dirty water, or with large bubbles), this assumption is based on the work of Lance (1986) who has shown that it is likely that the mean motion and pressure of the bubble and liquid are not affected by the bubble turbulence if

$$\epsilon V_t^2 \ll u_0^2,$$

where u_0 is a characteristic mean liquid velocity, and ϵ is the void fraction of bubbles.

Once the interfacial force F_i is determined, the motion of the bubble is related to F_i by Newtons' second law:

$$F_i = \rho_G V_b \left(\frac{dv_i}{dt} - g_i\right). \qquad [3c]$$

Classical calculations of the added mass coefficient C_m for simple bubble geometries at low Reynolds number have been made by Lamb (1932) and Milne-Thomson (1968). Other approaches to analyse added mass effects have been to include added mass terms in constitutive equations of motion for the bubble (Hinze 1962; Wallis 1969; Drew *et al.* 1979).

The approach used here is similar in principle to that of Cook & Harlow (1984) in that the two-phase flow field is taken to consist of three different flow fields: the bulk liquid far away from the bubble, the displaced liquid around the bubble and the bubble itself. Cook & Harlow introduce relationships between the three fields in terms of a parameter which is a fixed ratio of the void fraction of the displaced liquid to the volume fraction of the bubble. In this work the three fields are related in terms of the added mass coefficient C_m.

The practical advantages of working with three velocity fields are:

(i) The empirical relationships between relative velocity, void fraction and the terminal rise velocity can be replaced by a theoretical expression which can then be used in non-uniform flows with different bubble shapes.

(ii) The differences between the pressure near and far from the bubbles can be analysed, so that rational estimates can be given of the average liquid pressure, the wall pressure and the interstitial pressure far from the bubbles. These differences are of the order of the void fraction, and depend on the relative velocity between the bubbles and the liquid. They do not seem to have been analysed previously.

There have been several investigations in the determination of pressure loss in two-phase gas–liquid flows in pipes and fittings. Spedding *et al.* (1982) give an extensive review of the work carried out in two-phase flow pressure loss in inclined pipes. In general, the pressure drop due to resistance caused by the presence of particles is of interest, since flows of fluids through beds composed of stationary granular particles is a frequent occurrence in the chemical industry (Coulson *et al.* 1978). There has therefore been a great deal of work on engineering formulations

of pressure forces (Wallis 1969; Spalding 1980; Lewis & Davidson 1985). Such work is limited, however, in that the models use representations of pressure terms which do not seem to us to be physically correct. Prosperetti & Jones (1984) have presented a more rigorous analysis of pressure forces in disperse two-phase flow in which the pressure term is considered to be a combination of several different terms associated with average pressure, pressure drag and added mass forces, and rapidly varying components of pressure. A feature of their analysis with which we disagree is that their calculation of the pressure field is not based on a local analysis of the flow around the bubbles. In a similar approach we attempt to interpret the pressure forces in terms of the forces acting on the bubbles.

The final section of this paper is a theoretical analysis of two-phase acclerating flow in an inclined linear nozzle. The effect of void fraction on the variation of liquid velocity and bubble velocity through the nozzle is investigated. A prediction of two-phase pressure drop for the nozzle is compared with the experimental results of Lewis & Davidson (1985).

2. THE EFFECT OF PARTICLES ON FLUX OF FLUID

The general problem under consideration is the motion of a single air bubble in a liquid whose diameter is less than the length scales of the inhomogeneities in the flow. The bubble velocity is then $\mathbf{v}$ and the liquid velocity $\mathbf{u}_0$ is defined as that of the unperturbed fluid far from the bubble, for a flow containing several bubbles $\mathbf{u}_0$ would be the velocity of the undisturbed fluid between the bubbles ("interstitial" velocity), as illustrated in figure 1. By using this definition, rather than a definition based on the velocity averaged over the liquid volume, the dynamics of the bubble can be more easily calculated when there is a small but finite void fraction.

Darwin (1953) showed that in the potential flow of a sphere through a stationary fluid a mass of liquid is displaced equal to the hydrodynamic or virtual mass. Darwin defined this as the drift volume of fluid and calculated the trajectories of the particles of displaced fluid. In his idealized problem a solid body of volume V which is moving uniformly through an infinite incompressible fluid at rest passes through a thin plane P of fluid at right angles to the motion [the problem is addressed more formally by Brooke-Benjamin (1986)]. After the body has passed far beyond this plane the displaced surface and the initial plane encloses a drift volume $C_m V$ of fluid, as illustrated schematically in figure 2. If the bubbles move with a component of velocity v and the liquid moves at u, the number of bubbles passing relative to the liquid through a unit area at right angles to the flow is $\epsilon(v-u_0)/V$. Therefore the total liquid transported in unit time across a surface area A is

$$u_L A = [\underbrace{u_0(1-\epsilon)}_{\substack{\uparrow \\ \text{flux far} \\ \text{from} \\ \text{bubble}}} + \underbrace{C_m \epsilon(v-u_0)}_{\substack{\uparrow \\ \text{flux near} \\ \text{bubble}}}]A. \qquad [4]$$

In a three-dimensional steady flow this is generalized to

$$\frac{\partial}{\partial x_i}[u_{0i}(1-\epsilon) + C_m \epsilon(v_i - u_{0i})] = 0, \qquad [5]$$

where u_L is the *superficial liquid velocity* and u_{0i} is the velocity of the unperturbed fluid far away from the bubbles.

Note that $u_L > u_0$ if $C_m v > (1 + C_m)u$. This result is similar to the ideas discussed by Noordzij (1973). In one limiting case [4] describes the flux of a given volume of marked fluid in a flow containing a void fraction of particles which are stationary in the flow ($v = 0$), as illustrated in figure 3a. The flux is less than the volume flow rate of liquid $u_0(1-\epsilon)A$ because of entrapment of fluid by the particles, by a factor $C_m\epsilon/(1-\epsilon)$. The other limiting case is $u_L = 0$, which is the flow of bubbles rising in an ambient fluid. In this case [4] gives the negative (downward) flux of the fluid, which compensates for the motion of the bubbles (figure 3b).

The essence of [4] and [5] is that they contain the velocity of the gas phase *relative* to the local unperturbed liquid velocity between the bubbles. When spatial averages are used this connection

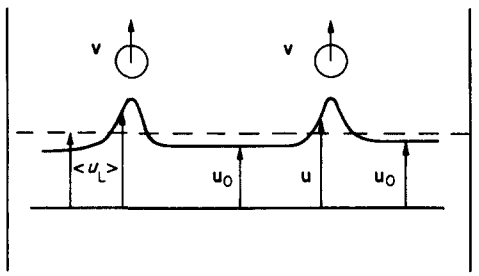

Figure 1. Definition sketch of the local liquid velocity **u** and bubble velocity **v** in disperse two-phase flow at low void fraction. The phase average velocity $\langle u_L \rangle$ and the effective interstitial velocity $\mathbf{u}_0$ far from the bubbles are also shown.

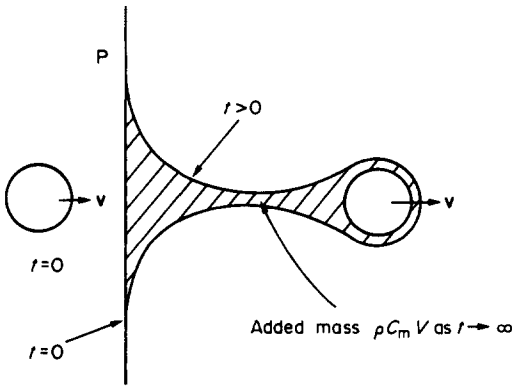

Figure 2. Illustration of the passage of a solid body through a plane P perpendicular to its path. The vertical line denotes a surface of material elements in the flow at $t = 0$ and the deformed surface at a later time (t). The hatched area is a volume that tends to $C_m V$ as $t \to \infty$.

is absent. The conservation laws for two-phase flows are usually given as phase averaged velocities $\langle u_L \rangle$ and $\langle v \rangle$ for the liquid and gas:

for the liquid in a one-dimensional flow,

$$(1-\epsilon)\langle u_L \rangle A = \text{const:} \qquad [6]$$

for the gas in one and three dimensions,

$$u_G A = \epsilon \langle v \rangle A = \text{const} \quad \text{and} \quad \frac{\partial}{\partial x_i}(\epsilon \langle v_i \rangle) = 0. \qquad [7]$$

It is more usual in two-phase flow calculations, following Zuber & Findlay (1965), to relate the bulk liquid and gas velocities u_L and u_G, by an empirical relation involving the void fraction ϵ and the bulk relative velocity $\langle V_s \rangle$, viz.

$$\frac{u_G}{\epsilon} = C_0(u_G + u_L) + \langle V_s \rangle, \qquad [8]$$

where C_0 is a coefficient representing the distribution of the dispersed bubbles relative to the liquid velocity profile. (There may well be other explanations.) In the case of a flat velocity profile and a uniform distribution of bubbles then $C_0 = 1$. In other cases, C_0 can be as high as 1.6. $\langle V_s \rangle$ is a weighted drift velocity which for laminar bubbly flow is given by (Govier & Aziz 1982, p. 383)

$$\langle V_s \rangle = C\left(\sigma g \frac{\Delta\rho}{\rho_L}\right)^{0.25}(1-\epsilon)^{1.5}. \qquad [9a]$$

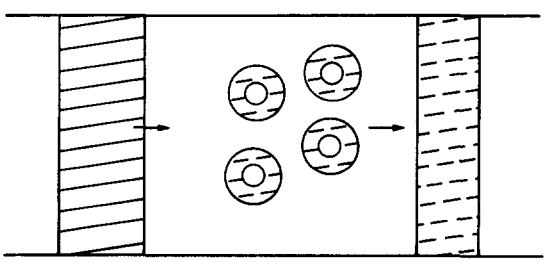

Figure 3a. Sketch of entrapment of marked fluid by stationary particles in a flow. The solid line denotes the initial marked fluid, the dashed line denotes the marked fluid law.

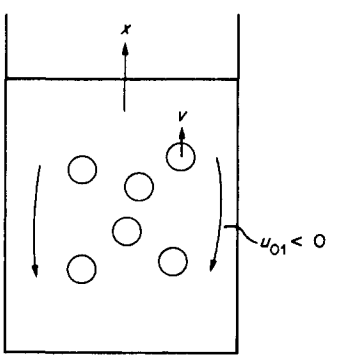

Figure 3b. Bubbles rising in an ambient fluid with a downward and opposite flux of fluid (i.e. a negative interstitial velocity $u_{01} < 0$), given by [4] with zero net upward flux (i.e. $\langle u_i \rangle = 0$).

Since $C(\sigma g \Delta\rho/\rho_L)^{0.25}$ is Harmathy's empirical relationship for V_t, the low void fraction equation [9a] can be re-expressed in our notation as

$$\langle V_s \rangle = V_t(1-\epsilon)^{1.5} \approx V_t(1-1.5\epsilon). \qquad [9b]$$

Substituting [9b] into [8], taking $C_0 = 1$, [8] reduces to

$$u_L\epsilon - u_G(1-\epsilon) = (-\epsilon + 1.5\epsilon^2)V_t. \qquad [10]$$

This *empirical* result can be compared with the *theoretical* predictions from [4] and [7], which when they are combined to eliminate the interstitial velocity, lead to

$$u_L\epsilon - u_G(1-\epsilon) = [-\epsilon + (1+C_m)\epsilon^2](v-u_0). \qquad [11]$$

Comparing [11] with [10] we see that the theoretical approach is consistent with Zuber & Findlay's (1965) empirically verified formulation if $v - u_0 = V_t$, and if $C_m = 0.5$. This confirms our view that the correct way to formulate drift velocity or slip is relative to the interstitial velocity. Void fraction does not then affect the bubble rise velocity directly. The Zuber & Findlay formulation masks the true effects of void fraction by considering the slip relative to the mean liquid velocity which has no physical significance for the bubbles.

3. PRESSURE GRADIENTS IN BUBBLY FLOW

3.1. A single particle in a control volume

In order to calculate the pressure gradient induced by bubbles and particles in non-uniform flows it is first necessary to relate the forces acting on a general particle in that flow to the pressures and stresses on a control volume far from the particle. Consider a particle with a surface denoted by β with an outward unit normal $\mathbf{n}_\beta$ to an element of this surface, moving with a velocity $\mathbf{v}$. The particle is enclosed within a bounding surface ξ with unit normal $\mathbf{n}_\xi$, see figure 4. The *total* volume of the fluid and particle is V, the fluid volume is V_f, and the particle volume is V_b. The fluid within this control volume is acted on by the forces as the control surface ξ and by the forces at the body surface β. On integration of the Navier–Stokes equation in tensor notation over the volume of fluid contained between the two surfaces, we have

$$\int\left(\frac{\partial p}{\partial x_i} + \rho_L\frac{\partial u_i}{\partial t} + \rho_L\frac{\partial}{\partial x_j}(u_iu_j) - \eta\frac{\partial^2 u_{0i}}{\partial x_j^2} - \rho_L g_i\right)\mathrm{d}V = 0, \qquad [12]$$

where p is the pressure and η is the viscosity. Using the divergence theorem, [12] implies

$$\int_\xi pn_i\,\mathrm{d}S - \int_\beta pn_i\,\mathrm{d}S + \rho_L\int_{V_f}\frac{\partial u_i}{\partial t}\,\mathrm{d}V + \int_\xi u_iu_jn_j\,\mathrm{d}S - \int_\beta u_iu_jn_j\,\mathrm{d}S$$
$$+\eta\int_\beta\frac{\partial u_i}{\partial x_j}n_j\,\mathrm{d}S - \eta\int_\xi\frac{\partial u_i}{\partial x_j}n_j\,\mathrm{d}S - \rho_L\int_{V_f} g_i\,\mathrm{d}V = 0. \qquad [13]$$

In order to use [13] to calculate the *change* in pressure caused by a particle, we need to consider the pressure gradient in the absence of the particle:

$$\frac{\partial p_0}{\partial x_i} + \rho_L\frac{\partial u_{0i}}{\partial t} + \frac{\partial}{\partial x_j}(\rho_L u_{0i}u_{0j}) - \eta\frac{\partial^2}{\partial x_j^2}u_{0i} - \rho_L g_i = 0, \qquad [14]$$

where the subscript "0" denotes values in the unperturbed fluid far away from the bubble. The control surface ξ is far enough from the particle that its perturbations on the undisturbed fluid velocity and pressure are small. Thus on ξ

$$u_i = u_{0i} + \Delta u_i, \quad p = p_0 + \Delta p, \quad \text{where} \quad |\Delta u_i| \ll |u_{0i}|, \quad |\Delta p| \ll |p_0|. \qquad [15]$$

Since there is no flux of fluid through the particle, the normal velocity in the fluid is equal to that in the liquid and therefore

$$u_jn_j = v_jn_j \quad \text{and} \quad \int_\beta u_iu_jn_j\,\mathrm{d}S = v_j\int_\beta u_in_j\,\mathrm{d}S. \qquad [16a]$$

If the particle is rigid, so that the no slip condition applies, $u_j = v_j$ and then

$$\int_\beta u_i u_j n_j \, dS = \int_\beta v_i v_j n_j \, dS = 0. \quad [16b]$$

Obviously, [16b] is a special case of [16a]. The viscous stresses τ_{ij} on the particle are defined by

$$\int_\beta \tau_{ij} n_j \, dS = \eta \int_\beta \frac{\partial u_i}{\partial x_j} n_j \, dS. \quad [17]$$

By integrating [14] within V_f, in the absence of the bubble, and using the results of [15]–[17], [13] leads to the interfacial force F_i being given in terms of the momentum flux across the control surface *and* the momentum of the liquid accelerating with the bubbles:

$$-(F_i - F_{0i}) = \int_\beta (p - p_0) n_i \, dS - \int_\beta (\tau_{ij} - \tau_{ij0}) n_j \, dS = \int_\xi \Delta p n_i \, dS + \rho_L \int_\xi (u_{0i} \Delta u_j + u_{0j} \Delta u_i) n_j \, dS$$

$$+ \rho_L \left\{ \int_{V_f} \frac{\partial (u_i - u_{0i})}{\partial t} \, dV - v_j \int_\beta u_i n_j \, dS + u_{0j} \int_\beta u_{0i} n_j \, dS \right\}, \quad [18]$$

where F_i is the i-component of the force acting *on the particle* given by [3a]. We have verified this formula by integrating the solution of the pressure and velocity field for a single bubble over the surface ξ.

The formulae [13] and [18] can be simplified for small symmetrical particles, namely a circular cylinder or a sphere in two- or three-dimensional flows in an *inviscid* straining flow. Then the integral of the change in $(\partial u_i / \partial t)$ over the fluid volume is

$$\int_{V_f} \frac{\partial (u_i - u_{0i})}{\partial t} \, dV = C_m V_b \left(\frac{dv_i}{dt} - \frac{\partial u_{0i}}{\partial t} \right). \quad [19a]$$

The surface integral over the particle in this case is also related to the non-uniformity of the ambient flow for a circular cylinder or sphere

$$v_j \int_\beta u_i n_j \, dS = V_b v_j \frac{\partial}{\partial x_j} u_{0i}. \quad [19b]$$

Substituting [19a] and [19b] into [18] leads to

$$-(F_{1i} - F_{0i}) = \int_\xi (\Delta p n_i + \rho_L (u_{0i} \Delta u_j + u_{0j} \Delta u_i) n_j) \, dS$$

$$+ \rho_L V_b \left[C_m \left(\frac{dv_i}{dt} - \frac{\partial u_{0i}}{\partial t} \right) - v_j \frac{\partial u_{0i}}{\partial x_j} + u_{0j} \frac{\partial u_{0i}}{\partial x_j} \right]. \quad [20a]$$

For some problems it is simpler to consider the *total* volume V within the surface ξ by including the liquid and the particle volume. Then using [19a] and [19b], [13] reduces to

$$\int_\xi (p n_i + \rho_L u_i u_j n_j) \, dS = -\int_V \left(\rho_L \frac{\partial u_{0i}}{\partial t} - g_i \right) dV - F_{1i} - \rho_L V_b \left[C_m \left(\frac{dv_i}{dt} - \frac{\partial u_{0i}}{\partial t} \right) - v_j \frac{\partial u_{0i}}{\partial x_j} + g_i \right]. \quad [20b]$$

This result has been checked by calculating the far field pressure and velocity around a sphere and a cylinder moving in an inviscid straining flow. (It is important to note that the far field pressure is unsteady because the particle moves through the non-uniform flow.).

3.2. A control volume containing many particles

We now consider the average pressure in the liquid for a bubbly flow containing *many* (N) *particles* ($n = 1, \ldots, N$), see figure 5, some of which are *close* to or *intersecting* the control surface ξ. So we need to consider the *average* over all possible locations and orientations of bubbles relative to this control surface. Evaluating this average is straightforward if we define the velocity and pressure in terms of their values *near* the particles (u_i and p). We make the *assumption* that the length scale of the control volume L is large compared with the distance between the bubbles which is of order $a\epsilon^{-1}$, a is a typical bubble diameter. Then the contributions to the volume integrals are

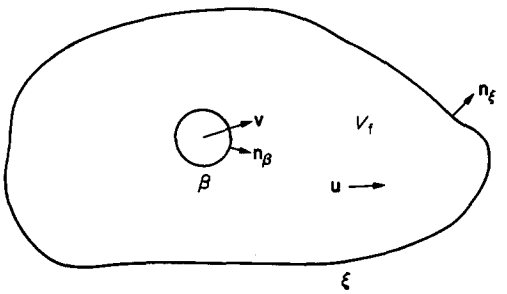

Figure 4. Definition sketch for the calculation of momentum flux through a control surface ξ of a liquid volume V_f, containing a single bubble with surface β.

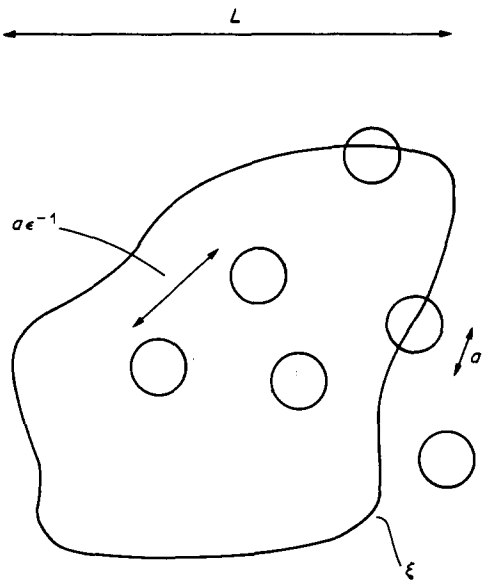

Figure 5. Definition sketch of a control volume of length scale L containing many particles of radius a. Note that L is much greater than the average distance between particles (of order $a\epsilon^{-1}$).

independent of the averaging operation of $u_i u_j$ and p near the control surface. [One might describe this as a "fuzzy" control surface whose thickness is $O(a\epsilon^{-1})$, by analogy with the usual continuum approximation.]

We denote a volume average within the *liquid* alone by $\langle\ \rangle$, over a scale of order $a\epsilon^{-1}$. Note that, because the pressure and velocity field *near* the bubbles are different from their interstitial values, $\langle p\rangle \neq p_0$ and $\langle u_i u_j\rangle \neq u_{0i}u_{0j}$. Note that because the interstitial values of p and u_i are defined to be constant (locally on a scale $a\epsilon^{-1}$),

$$\langle p_0\rangle = p_0 \quad \text{and} \quad \langle u_{0i}u_{0j}\rangle = u_{0i}u_{0j}.$$

Then the integral of [20b] within the control surface ξ, when all N particles are considered, is

$$\int_\xi (p_0 n_i + \rho_L u_{0i}u_{0j}n_j)\,\mathrm{d}S + \int_\xi \delta M_i\,\mathrm{d}S = -\int_V \rho_L\left(\frac{\partial u_{0i}}{\partial t} - g_i\right)\mathrm{d}V - \sum_{n=1}^{N}\left[F_i^{(n)} - V^{(n)}\rho_L\left\{C_m\left(\frac{\mathrm{d}v_i^{(n)}}{\mathrm{d}t} - \frac{\partial u_{0i}}{\partial t}\right) - v_j\frac{\partial u_{0i}}{\partial x_j} + g_i\right\}\right], \quad [21a]$$

where δM_i is the additional momentum flux in the liquid at the control surface caused by the flow near the bubbles and by the viscous stress,

$$\delta M_i = -\int_\xi \left[(\langle p\rangle - p_0)n_i + \rho_L(\langle u_i u_j\rangle - u_{0i}u_{0j})n_i - \eta\frac{\partial u_{0i}}{\partial x_j}n_j\right]\mathrm{d}S. \quad [21b]$$

In inviscid flow, for bubbles at high Reynolds number, the differences between $\langle p\rangle$ and p_0 and between $\langle u_i u_j\rangle$ and $u_{0i}u_{0j}$ are caused by the additional kinetic energy and momentum flux in the liquid near the bubbles. These are proportional to the square of the difference between the velocity of the bubble u_i and that of the liquid surrounding the bubble u_{0i}. They are also proportional to the relative volume of the liquid occupied by the bubbles.

For spherical bubbles in irrotational flow (such that the gradients of u_{0i} are small over a scale a), potential theory (see appendix D) gives

$$\langle p\rangle - p_0 = -\frac{\frac{1}{2}C_m\rho_L(v_i - u_{0i})^2\epsilon}{(1-\epsilon)},$$

and

$$\rho_L(\langle u_i u_j\rangle - u_{0i}u_{0j}) = \frac{\frac{\lambda}{2} C_m \rho_L (v_i - u_{0i})^2 \delta_{ij}\epsilon}{(1-\epsilon)}, \quad [22]$$

where $\lambda = 4/5$.

The result in [21a] can be applied to the pressure drop along a duct (see figure 6), between cross-sections (1) and (2) at $x = x_1^{(1)}, x_1^{(2)}$ normal to the x_1-axis. The areas are $A^{(1)}$ and $A^{(2)}$. Note that over the area of the walls of the duct A_w the pressure, defined as p_w (to be discussed later), acts normal to the wall in the direction $-\mathbf{n}_w$. But the normal velocity is zero so $u_i n_{wi} = 0$. It is convenient to express the force on a particle as the average force on a particle per unit volume

$$\frac{\bar{F}_i}{V} = \frac{1}{N}\sum_1^N \frac{F_i^{(n)}}{V^{(n)}},$$

where V is the *average* volume of the particles, and the acceleration as

$$\overline{\frac{\partial v_1}{\partial t}} = \frac{1}{N}\sum_1^N \frac{dv_1^{(n)}}{dt}.$$

Since we are considering the local average of the added mass acceleration of many particles, it is necessary to write this differential as $\overline{\partial v/\partial t}$. Note that it implies that in the limiting case of the particles having the same density as the liquid $\rho_p = \rho_L$, then

$$v_1 = u_{01} \quad \text{and} \quad \frac{\partial u_{01}}{\partial t} = 0, \quad \int \frac{\partial}{\partial t}(u_i - u_{0i})\, dV = 0.$$

By considering the component of [21a] *along* the duct, we obtain:

$$\int_{A^{(1)}} (p_0 + \rho_L u_{01}^2 + \delta M_1)\, dA - \int_{A^{(2)}} (p_0 + \rho_L u_{01}^2 + \delta M_1)\, dA + \int_{A_w} p_w n_{w1}\, dA$$

$$= -\int_V \left\{\epsilon\left[\frac{\bar{F}_1}{V} + \rho_L C_m\left(\overline{\frac{\partial v_1}{\partial t}} - \frac{\partial u_{01}}{\partial t}\right) - \rho_L v_1 \frac{\partial u_{01}}{\partial x_1}\right] - (1-\epsilon)\rho_L\left(g_1 - \frac{\partial u_{01}}{\partial t}\right)\right\} dV, \quad [23a]$$

where

$$\delta M_1 = \tfrac{1}{2} C_m \rho_L \overline{(v_1 - u_{01})^2}(\lambda - 1)\epsilon(1-\epsilon), \quad [23b]$$

and λ is given by [22] for high Reynolds number for the bubbles.

By considering the two cross-sections at $x_1^{(1)}$ and $x_1^{(2)}$ to be close enough that the change in area A is small so $|A^{(1)} - A^{(2)}| \ll A^{(1)}$, but separate enough to be greater than the distance between the bubbles (i.e. $|x_1^{(1)} - x_1^{(2)}| \gg a\epsilon^{-1}$), and assuming that the flow and the bubble distribution is *uniform* across the section, and that the presssure on the walls is constant around the cross-section, it is possible to convert the control volume equation [23a] into a differential equation for the rate of change of p_0, u_{01} and A_1 in terms of F_1, ϵ, v_1 and $(\partial u_{01}/\partial t)$, viz.

$$\frac{d}{dx_1}[A(p_0 + \rho_L u_{01}^2 + \delta M_1)]$$

$$= p_w \frac{dA}{dx} - A\left\{\epsilon\left[\frac{\bar{F}_1}{V} + \rho_L C_m\left(\overline{\frac{\partial v_1}{\partial t}} - \frac{\partial u_{01}}{\partial t}\right) - \rho_L v_1 \frac{\partial u_{01}}{\partial x_1}\right] + \rho_L(1-\epsilon)\left(\frac{\partial u_{01}}{\partial t} - g_1\right)\right\} dV, \quad [24]$$

where δM_1 is given by [23b]. A useful check on these equations is that they show that an ensemble of particles with the same density (i.e. $\rho_p = \rho_L$) as the liquid, move at the same velocity (i.e. $v_1 = u_{0_1}$) as the liquid and lead to the same pressure as for a homogeneous flow.

Equations [3a] and [24] imply that the change of pressure and momentum flux is balanced by the force on the particles and effects of acceleration around the particles. We note immediately that in an accelerating flow, where $Du_{0_1}/Dt > 0$ and $(v_1 - u_{0_1}) > 0$, the result is that the pressure gradient is increased (in the case of a converging flow the negative pressure drop is increased).

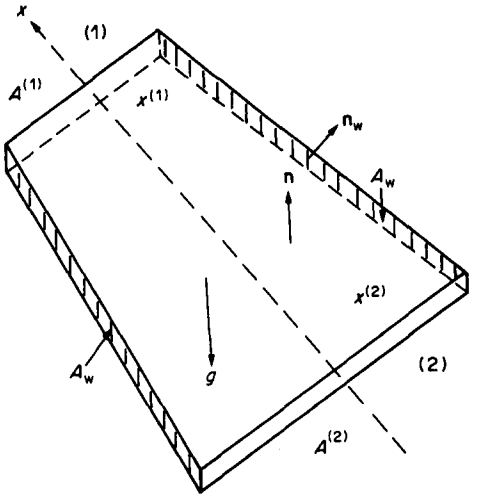

Figure 6. Flow through a duct from cross-section (2) to cross-section (1).

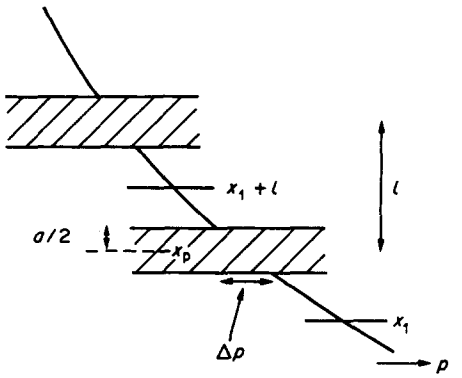

Figure 7. Sketch to show why the average pressure gradient in the liquid phase $\langle dp/dx \rangle$ is not equal to the bulk pressure gradient dp_b/dx. The particles are represented as slices across which there is a pressure drop Δp.

To understand what exactly is meant by this differentiation it is helpful to consider the simplest case of sedimenting particles in a stationary liquid. In this situation $(d/dx)\delta M_1 = 0$, and [24] reduces to the well-known result

$$\frac{dp_0}{dx_1} = -\epsilon \frac{F_1}{V} + \rho(1-\epsilon)g_1. \qquad [25]$$

In this case $g_1 = -g$, and from [3c] $F_1/V = \rho_p Vg$, so [25] reduces to

$$\frac{dp_0}{dx_1} = -g[\rho_L - \epsilon(\rho_L - \rho_p)]. \qquad [26]$$

In this case the interstitial pressure gradient is equal to the usual "bulk" pressure gradient dp_b/dx measured as a pressure difference between two planes over a distance large compared to $a\epsilon^{-1}$.

As G. K. Batchelor (unpublished) has pointed out, this "bulk" pressure gradient is *not* equal to the average pressure gradient *in the liquid*, $\langle dp/dx_1 \rangle$. For this case, the latter is equal to the average viscous force exerted on the liquid by the particles and is determined by the detailed flow around the particle.

A diagrammatic sketch (figure 7) shows why in general dp_b/dx_1 (which is approximately the pressure gradient on the walls of a container) is not equal to $\langle dp/dx_1 \rangle$. The particles (represented by slices of another phase) are equally spaced a distance l apart. These are represented by the shaded regions. Because of the equal spacing, the value of dp_b/dx_1 is equal to $[p(x_1 + l) - p(x_1)]/l$, but the average value of dp/dx just in the liquid, is given by the integral of dp/dx in the space *between* the particles

$$\left\langle \frac{\partial p}{\partial x_1} \right\rangle = \frac{1}{(l-a)} \int_{x_p + \frac{a}{2}}^{x_p + l - \frac{a}{2}} \frac{\partial p}{\partial x_1} dx_1.$$

Because there is a pressure difference Δp across the particle, there is a difference between dp_b/dx_1 and $\langle dp/dx_1 \rangle$ given by

$$\frac{dp_b}{dx_1} = \frac{\left[(l-a)\left\langle \frac{\partial p}{\partial x_1} \right\rangle + \Delta p\right]}{l}.$$

For the case of sedimenting spheres at low Reynolds number their effect on $\langle dp/dx_1 \rangle$ is two-thirds of their effect on dp_0/dx_1 (G. K. Batchelor, private communication).

4. BUBBLY FLOW IN A NOZZLE

The steady flow air and liquid in a converging nozzle is described here by a one-dimensional flow model. The section under consideration is a linear contraction in a pipe whose axis lies at an angle α to the vertical (figure 8). The cross-sectional area of the nozzle is given by

$$A(x) = \frac{x}{x_f} A_f + \left(1 - \frac{x}{x_f}\right) A(0), \qquad [27]$$

where $A(0)$, A_f and x_f are known, $x = 0$ is the position of the beginning of the contraction and $x = 9.5$ cm is the position of the throat. Consider the motion of an identical set of spherical, non-deformable air bubbles (dia < 3 mm) which are being acclerated by the flow but are undergoing only weak mutual interaction. In order to facilitate the analysis certain assumptions are made about the flow:

1. At a given cross-section of the flow all the bubbles move with the same velocity.
2. The axial gradients in velocity in the nozzle are of an order of magnitude greater than the transverse gradients.
3. The liquid is pure so that a linear drag law may be assumed ($f \equiv 1$ in [3]).
4. The axial component of the rise velocity for isolated bubbles in still liquid is $V_t \cos\alpha$, where $V_t = 25\ \text{cm s}^{-1}$ (Clift *et al.* 1978).
5. The density of a gas bubble is zero ($\rho_G = 0$).
6. The void fraction is low enough that the force on each bubble is independent of other bubbles.
7. To interpret wall pressure measurements we *assume* that the wall pressure p_w is equal to the average liquid pressure $\langle p \rangle$.

With these simplifications the expression for the force acting on a bubble in this one-dimensional flow reduces to

$$C_m v \frac{dv}{dx} = (1 + C_m) u_0 \frac{du_0}{dx} + g \cos\alpha - g \frac{v - u}{V_t} + O(\epsilon), \qquad [28]$$

where v is the axial component of the bubble velocity and writing u_0 for u_{0_l}, the interstitial liquid velocity. The correction to C_m is also of order ϵ (Van Wijngaarden 1976). Note that the lift term is identically zero in [28].

The set of three conservation equations for the three independent variables v, u and ϵ in this flow are [28] and the continuity equations

$$[u_0(1 - \epsilon) + C_m \epsilon (v - u_0)] A = \text{const} \qquad [29]$$

and

$$v \epsilon A = \text{const}. \qquad [30]$$

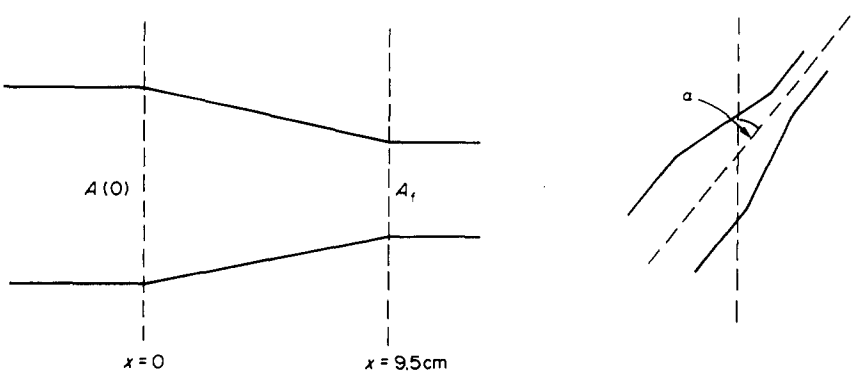

Figure 8. Sketch of a linear nozzle inclined at an angle α to the vertical.

For low values of ϵ the differential equation of motion and the mass conservation equations are solved using perturbation techniques to give the bubble and liquid velocities, the variation of void fraction through the nozzle, and the pressure drop in the contraction. The details of the mathematical procedure are given in appendix C.

In analysis of the computations it is instructive to consider the limiting solution of [28] when the acceleration effects are very large [i.e. $u_0(du_0/dx) \gg g$], only the inertial terms are significant and then

$$v^2 = 3[u_0^2 - u_0^2(0)] + v^2(0), \qquad [31]$$

so the bubbles accelerate much faster than the liquid. When the inertial terms are small

$$v = u_0 + V_t \cos\alpha, \qquad [32]$$

so that the bubbles move with the liquid velocity plus a relative velocity.

5. RESULTS

Figures 9 and 10 show the variation of bubble and liquid interstitial velocity through the contraction for a flow containing a single bubble. The graphs are drawn for three different angles of inclination of the nozzle to the vertical (0°, 45° and 90°) and for representative values of liquid velocity of 10 and 50 cm s^{-1}. The nozzle was taken to have a length $L = 9.5$ cm and an inlet diameter D_I and throat diameter D_n of 7.8 and 3.9 cm respectively, giving a contraction ratio of 4:1. Unless it is stated otherwise, these are taken to be the dimensions of the nozzle throughout the following analysis.

For a liquid velocity of 10 cm s^{-1} the computed profiles are shown in figure 9. The liquid velocity ($\times\times\times$) is seen to increase through the contraction from 10 to 40 cm s^{-1} and thereafter remains at 40 cm s^{-1}. This rather artificial profile is due to the assumed form of $A(x)$ in [27]. For the horizontal pipe ($\alpha = 90°$) there is no component of buoyancy and the terminal rise velocity is zero. The bubble is accelerated through the nozzle and the relative velocity ($v_0^{(0)} - u_0^{(0)}$) increases from 0 to 8 cm s^{-1}. On leaving the nozzle the bubble is acted on by drag and its velocity returns to that of the liquid. The pattern is repeated as α is decreased with the initial bubble velocity being that of the liquid plus the component of terminal rise velocity. Again, the relative velocity increases as the bubble passes through the contraction and then returns to its initial value.

For the higher liquid velocity of 50 cm s^{-1} a similar set of graphs is shown in figure 10, together with the inviscid solution of [C.5] for the case $\alpha = 0$ and in which Δu is large compared with V_t, given by [31]. It is seen ($***$) that when the inertial terms are significantly greater than the drag

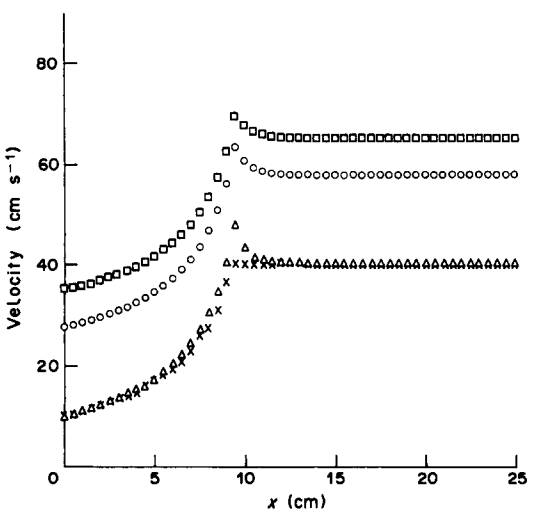

Figure 9. Bubble and liquid velocity profiles for a single bubble in a linear nozzle (the contraction ratio $C_R = 4$), calculated from [C.5] and [C.6] with $u_0^{(0)}(0) = 10$ cm s^{-1} and $V_t = 25 \cos\alpha$ cm s^{-1}. $u_0^{(0)}$: $\times$, $\alpha = 0°$, 45°, 90°. $v^{(0)}$: □, $\alpha = 0°$; ○, $\alpha = 45°$; △, $\alpha = 90°$.

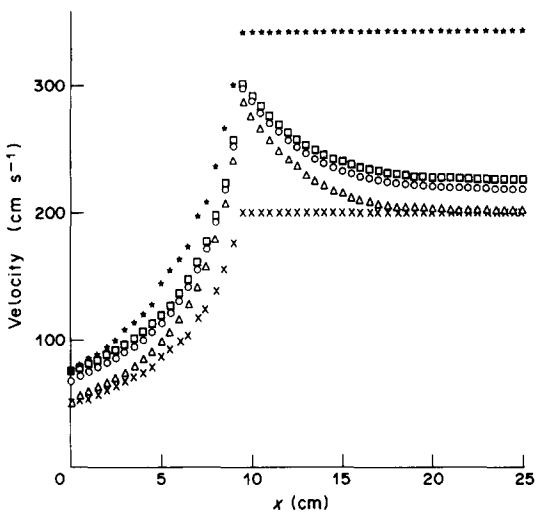

Figure 10. Bubble and liquid velocity profiles for a single bubble in a linear nozzle, calculated from [C.5] and [C.6] with $u_0^{(0)}(0) = 50\ \text{cm s}^{-1}$ and $V_t = 25 \cos\alpha\ \text{cm s}^{-1}$. $u_0^{(0)}$: ×: $\alpha = 0°$, 45°, 90°. $v^{(0)}$: □, $\alpha = 0°$; ○, $\alpha = 45°$; △, $\alpha = 90°$. $v_0^{(0)}$: *, $\alpha = 0°$ given by [31].

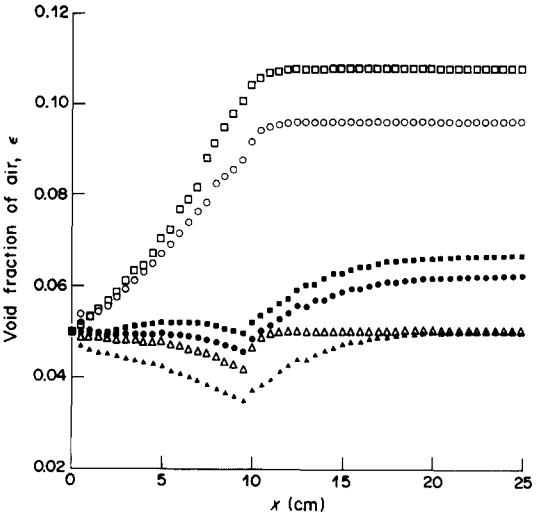

Figure 11. Variation of gas void fraction through a linear nozzle. Plots are for $\epsilon(0) = 0.05$. $u_0^{(0)}(0) = 10\ \text{cm s}^{-1}$: □, $\alpha = 0°$; ○, $\alpha = 45°$; △, $\alpha = 90°$. $u_0^{(0)}(0) = 50\ \text{cm s}^{-1}$: ■, $\alpha = 0°$; ●, $\alpha = 45°$; ▲, $\alpha = 90°$.

on the bubble its velocity increases in the nozzle and thereafter continues to move at the velocity it attains at the nozzle throat. Now introducing more bubbles so that the initial void fraction $\epsilon(0) = 0.05$, figure 11 shows the variation of gas void fraction with distance from the nozzle inlet. It is clear that there is a significant variation of ϵ for the two different initial velocities $u_0^{(0)}(0)$ and that for both values of $u_0^{(0)}(0)$ the change in void fraction in the horizontal pipe ($\alpha = 90°$) has a similar behaviour. In fact the behaviour of ϵ, when $\epsilon \ll 1$, may be predicted analytically by writing [C.9] in the form

$$\frac{\epsilon}{\epsilon(0)} = \frac{v_0^{(0)}(0)}{u_0^{(0)}(0)}\left(1 - \frac{v^{(0)} - u_0^{(0)}}{v^{(0)}}\right), \qquad [33]$$

using [C.6]. It follows immediately from [33] that for $\alpha = 90°$, in which $v^{(0)}(0) = u_0^{(0)}(0)$, that there is no initial slip between the phases, so that $\epsilon = \epsilon(0)$. Beyond the throat of the nozzle $v^{(0)} = u_0^{(0)}$ because of drag, so again the void fraction returns to the inlet value. At the throat of the nozzle ($x = 9.5$ cm) the relative velocity $(v^{(0)} - u_0^{(0)})$ is a maximum; hence $\epsilon/\epsilon(0)$ has a minimum which is < 1 for all liquid velocities. The case when $\alpha \neq 90°$ is interesting in that the initial behaviour of $\epsilon/\epsilon(0)$ is dependent on the value of $u_0(0)$. For both velocities, ϵ increases from $\epsilon(0)$ downstream of the throat because $(v^{(0)} - u_0^{(0)})$ returns to the constant value $V_t \cos\alpha$ because of drag, and $v^{(0)}$ has increased. Near $x = 0$ the behaviour of $\epsilon/\epsilon(0)$ is governed by the relative increase of bubble velocity $v^{(0)}$ and slip $(v^{(0)} - u_0^{(0)})$, with the bubble velocity for $u_0^{(0)}(0) = 10\ \text{cm s}^{-1}$ increasing more rapidly than the slip and vice versa for $u_0^{(0)}(0) = 50\ \text{cm s}^{-1}$. This is also reflected in the behaviour of ϵ at the throat of the nozzle.

It appears, on all plots of $\epsilon/\epsilon(0)$, that the void fraction does not settle down to a constant value immediately at the throat of the nozzle, in some cases not until values of x relatively far downstream of the throat. The reason is that the drag effect takes a finite distance $\approx aC_D 10u_0^{(0)}/(v^{(0)} - u_0^{(0)})_{\text{throat}}$ to bring the relative velocity back to 10% of its initial value $V_t \cos\alpha$ after the bubbles clear the throat of the nozzle. Similar observations have been made by Thang & Davis (1979), who measured profiles of void fraction across vertical venturi tubes at different points along the nozzle. They measured an increase in mean void fraction through the venturi which is consistent with the plots in figure 11 with $\alpha \neq 90°$. The variation of void fraction is similar for other values of $\epsilon(0)$.

Figure 12 shows the effect of the variation of void fraction through the nozzle on the liquid interstitial velocity u_0 for $u_0^{(0)}(0) = 10\ \text{cm s}^{-1}$ and $\epsilon(0) = 0.05$ and 0.1. The plots are drawn for $\alpha = 0°$ and 90° only for the sake of clarity. It is shown that for a given value of α and $\epsilon(0)$ there is an increase in the value of liquid velocity from the value $u_0^{(0)}$ at a given position in the nozzle. The

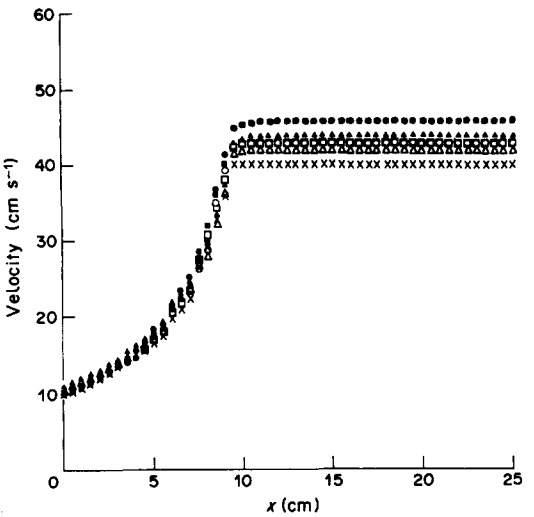

Figure 12. Effect of void fraction on liquid velocity in a linear nozzle. Plots are for $u_0^{(0)}(0) = 10\ \text{cm s}^{-1}$. $\epsilon(0) = 0$: ×, $\alpha = 0°$, $90°$. $\epsilon(0) = 0.05$: □, $\alpha = 0°$; △, $\alpha = 90°$. $\epsilon(0) = 0.1$: ■, $\alpha = 0°$; ▲, $\alpha = 90°$.

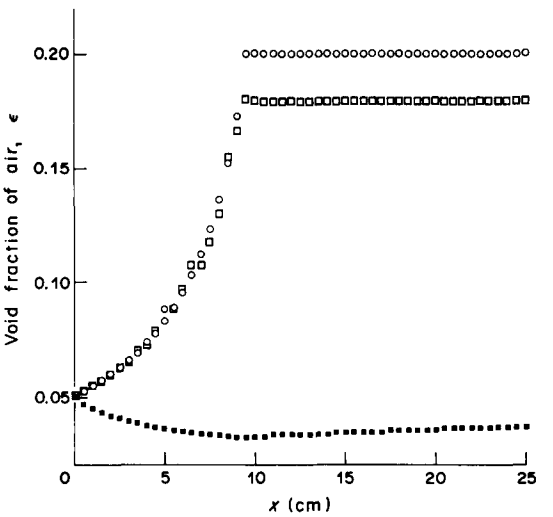

Figure 13. Effect of void fraction on liquid velocity in a vertical linear nozzle for limiting cases of terminal rise velocity. Plots are for $\epsilon(0) = 0.05$ and $V_t = 25\ \text{cm s}^{-1}$. □, $u_0^{(0)}(0) = 1\ \text{cm s}^{-1}$; ■, $u_0^{(0)}(0) = 500\ \text{cm s}^{-1}$; ○, limiting case for $u_0^{(0)}(0) = 1\ \text{cm s}^{-1}$.

value of ϵ increases on passing through the contraction so that the effective cross-sectional area through which the liquid has to pass decreases, so the liquid velocity has to increase to maintain a constant flow rate through the nozzle. Note that from [C.1] and [C.8] the initial interstitial velocity is $(10 + 0.1 \times \frac{1}{2}) = 10.05$, in the horizontal nozzle ($\alpha = 90°$), where the void fraction ϵ does not change, the final liquid interstitial velocity is about four times its initial value.

Figure 13 shows the variation of void fraction in a vertical nozzle for two limiting cases of terminal rise velocity. For the case $V_t \gg u_0$, so that $v \approx V_t$, ($V_t \approx 25\ \text{cm s}^{-1}$), [7] predicts that the variation of ϵ through the nozzle is approximated by $\epsilon = \epsilon(0)\, A(0)/A$(○○○). It is seen from the plot for $u_0^{(0)}(0) = 1\ \text{cm s}^{-1}$ (□□□) that this limit is approached. For $V_t \ll u_0$, [31] gives $v \approx \sqrt{3}u_0$, [4] and [7] then imply that the limiting value of ϵ is $\epsilon(0)/\sqrt{3}$, which is confirmed by the plot for $u_0^{(0)}(0) = 500\ \text{cm s}^{-1}$ (■■■).

A comparison between the graphs in figure 10 with those in figures 14 and 15 shows the effect on v of increasing the number of bubbles in the flow. It is seen that for a given value of α, at a fixed position in the nozzle, the effect of increasing $\epsilon(0)$ is to increase v. This is most noticeable at the throat of the nozzle where the absolute value of slip $(v - u_0)$ has increased, remembering that u_0 has also increased with $\epsilon(0)$. The liquid velocity profile for $\alpha = 90°$ only is shown. For $\epsilon \neq 0$ it is evident from figures 14 and 15 that the bubble velocity does not settle to a constant value until a relatively far distance downstream of the throat, in comparison to the plots in figure 10. This is a result of the void fraction taking a finite time to adjust itself to a constant value on leaving the contraction, as was noted in figure 11. It is also noted that the final values of v downstream have increased since the final values of liquid velocity have increased (see figure 12), and $v = u + V_L \cos\alpha$ for large x.

Figure 16 shows the plots of the pressure terms. The graphs for $\alpha = 90°$ only are shown, for clarity. Also drawn for comparison is the pressure variation for liquid flow only through the nozzle [$\epsilon(0) = 0$]. The graphs show that the average pressure in the liquid between the bubbles p_0 is approximately the same as the average pressure $\langle p \rangle$ across the whole liquid. We assume $p_w \approx \langle p \rangle$, since bubbles move near the wall. A comparison between the graph of p_w and the graph of pressure p, for $\epsilon(0) = 0$, shows that the effect of the presence of a void fraction of bubbles is to increase the pressure drop through the nozzle. The continuing decrease in pressure drop downstream of the throat is due the hydrostatic head, though for p_w this may also be due to the adjustment of the void fraction as noted in figure 11. It is of interest to note that p_w is the pressure which a measuring device such as a pressure transducer would register.

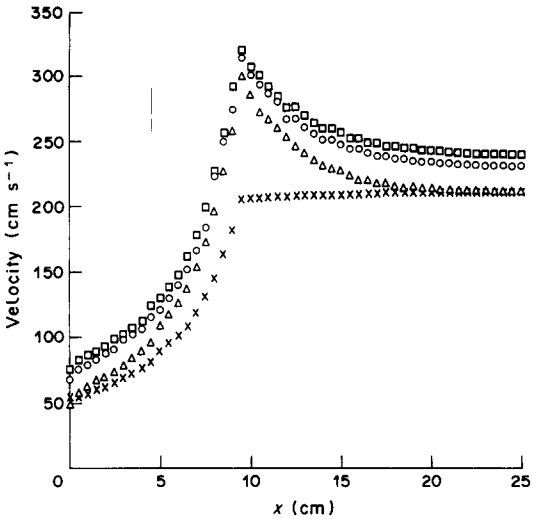

Figure 14. Bubble and liquid velocity profiles for a dilute concentration of bubbles in a linear nozzle, calculated from [C.5]–[C.9] with $u_0^{(0)}(0) = 50\ \text{cm s}^{-1}$, $V_t = 25 \cos\alpha\ \text{cm s}^{-1}$ and $\epsilon(0) = 0.05$. u: ×, $\alpha = 0°$, 45°, 90°. v: □, $\alpha = 0°$; ○, $\alpha = 45°$; △, $\alpha = 90°$.

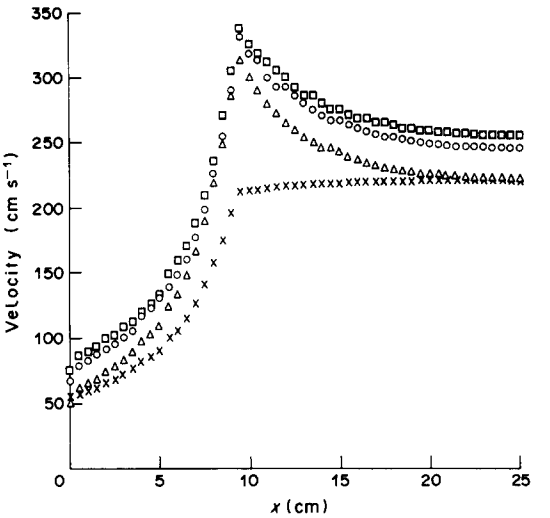

Figure 15. Bubble and liquid velocity profiles for a dilute concentration of bubbles in a linear nozzle, calculated from [C.5]–[C.9] with $u_0^{(0)}(0) = 50\ \text{cm s}^{-1}$, $V_t = 25 \cos\alpha\ \text{cm s}^{-1}$ and $\epsilon(0) = 0.1$. u: ×, $\alpha = 0°$, 45°, 90°. v: □, $\alpha = 0°$; ○, $\alpha = 45°$; △, $\alpha = 90°$.

Figure 17 shows the comparison between the theoretical results discussed in section 5 and the experimental data of Lewis & Davidson (1985) for the variation of two-phase pressure drop with gas void fraction for a converging nozzle for different superficial liquid velocities and different values of inlet and throat area. Lewis & Davidson measured the ratio of two-phase pressure drop at the throat Δp with the equivalent pressure drop Δp_{L0} for liquid flow only. This ratio was plotted against the *upstream* gas void fraction $\epsilon(0)$, the superficial velocity having the same value at each value of $\epsilon(0)$.

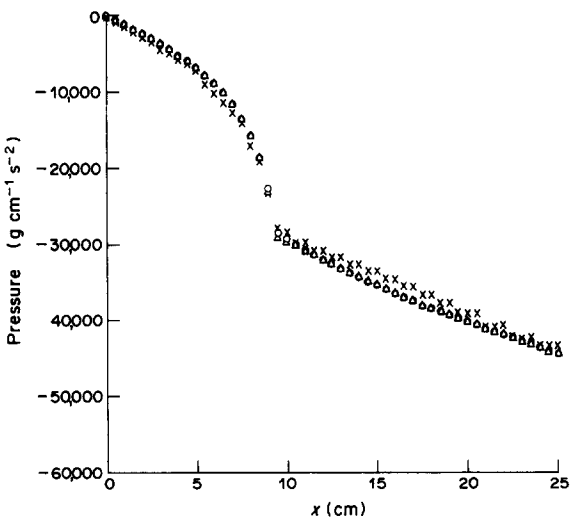

Figure 16. Plots of pressure variation in a vertical linear nozzle, calculated from [B.4]–[B.6] with $u_0^{(0)}(0) = 50\ \text{cm s}^{-1}$ and $V_t = 25\ \text{cm s}^{-1}$. $\epsilon(0) = 0$: ×, p_{L0}. $\epsilon(0) = 0.1$: ○, p_0; △, p_w.

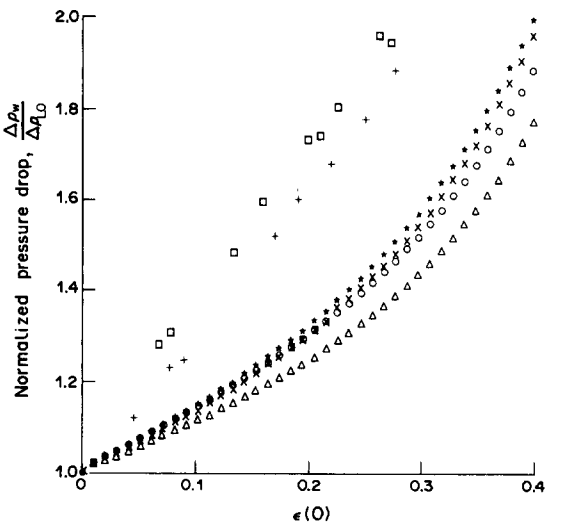

Figure 17. Comparison of theoretical analysis of the ratio of pressure drop with and without bubbles for the same liquid flow rate in a vertical nozzle with the measurements of Lewis & Davidson (1985). (Here it is assumed that there is a relative velocity at the surface of the bubbles). $D_n = 3$ cm, $C_R = 10$, $L = 0.9$ cm, $u_L = 52\ \text{cm s}^{-1}$: □, experiment; ×, theory. $D_n = 4$ cm, $C_R = 10$, $L = 1.2$ cm, $u_L = 54\ \text{cm s}^{-1}$: +, experiment, *, theory. $D_n = 3$ cm, $C_R = 5.7$, $L = 0.9$ cm, $u_L = 52\ \text{cm s}^{-1}$: △, theory. $D_n = 4$ cm, $C_R = 5.7$, $L = 1.2$ cm, $u_L = 54\ \text{cm s}^{-1}$: ○, theory.

In their apparatus, nozzles with entrance diameters D_E of 4.5 and 6 cm and throat diameters D_N of 3 and 4 cm, respectively, were mounted in the centre of a 9.52 cm dia ($=D_I$) pipe and pressure measurements were taken between transducers positioned one diameter D_I upstream of the entrance to the nozzle, and at a distance $H = 14.28$ cm ($=1.5D_I$) downstream of this point. In the theoretical model we assume a linear nozzle with an inlet diameter D_I of 9.52 cm and throat diameters of 3 and 4 cm, giving contraction ratios $C_R = A(0)/A(L)$ of 10 and 5.7, respectively. The lengths of the nozzles were taken to be $L = D_I + 0.304D_N$, and thereafter the nozzle becomes a straight pipe of diameter D_N. The pressure difference is measured from the entrance of the nozzle to a distance 14.28 cm downstream. The hydrostatic pressure difference in the nozzle is taken into consideration in [B.6]. Lewis & Davidson add a correction factor $\epsilon(H)\rho gH$ to their measured pressure drop to account for the hydrostatic pressure difference due to the difference in height between the transducers.

In figure 17, in order to make a valid comparison with the Lewis & Davidson data, we plot the ratio $\Delta p/\Delta p_{L0}$ vs $\epsilon(0)$ for the nozzle where $\Delta p = \Delta p_w - \epsilon(H)\rho gH$, Δp_w is our calculated pressure drop and $\epsilon(H)$ is our theoretical value of downstream void fraction. Figure 17 shows that where ϵ is small the ratio is linear in ϵ, and the agreement is reasonable given that the above analysis assumed a different type of nozzle from that of Lewis & Davidson (though we have checked that the nozzle shape does not greatly affect the results) and we have made certain assumptions about nozzle specifications in the model. Note that the theory is only valid to $O(\epsilon)$, so the non-linear element of the curve cannot be trusted.

Simplistic assumptions might lead one to expect that for a fixed value of superficial velocity the pressure drop would decrease as $\epsilon(0)$ increases, when in fact the pressure drop is seen to increase. A consideration of the flow as two separate liquid and gas phases explains why this is so. From a simple mass balance for the liquid, as $\epsilon(0)$ increases the liquid has effectively a smaller cross-sectional area through which to pass and its velocity (and therefore pressure drop) necessarily increases. This assumes that the bubbles are small enough not to become elongated in the contraction.

In the derivation of [B.6] it was assumed that the flow was inviscid and slipped over the surfaces (e.g. small spherical bubbles in pure liquid). However, for a particle such as a bubble in a real liquid the flow is closer to that over a rigid particle with a *no-slip* condition and a significant drag, then [16b] rather than [19b] is relevant and the term in [B.5] $[=\rho_L v_l(\partial u_{0l}/\partial x_l)]$ has to be omitted. The resulting plots in figure 18 are drawn for the same parameter values as in figure 17. With the slip

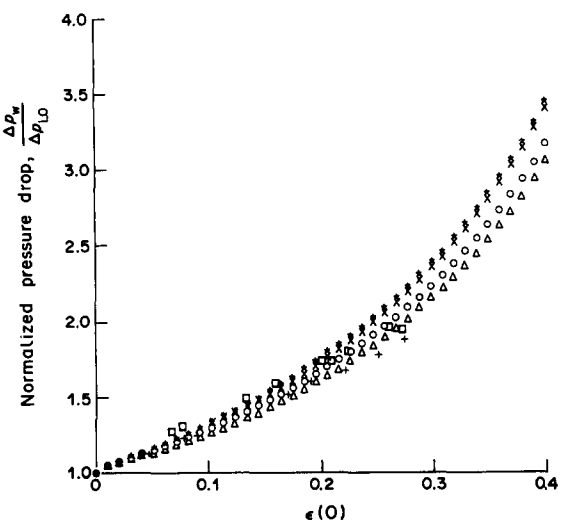

Figure 18. Plots of pressure drop for the same parameter values as in figure 17, assuming that the bubbles have rigid surfaces so that a slip condition is applied.

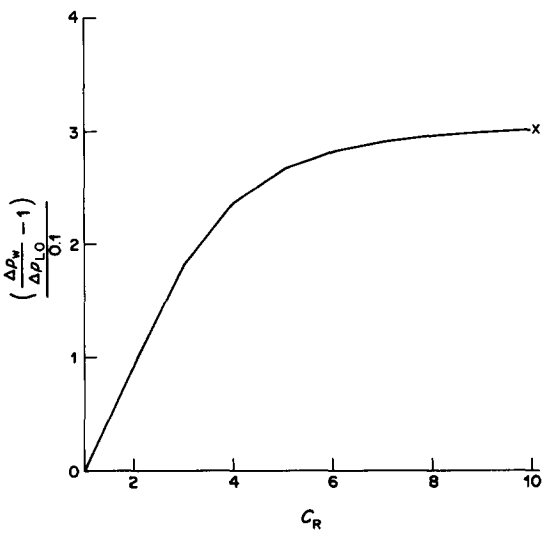

Figure 19. Plot of the difference between the pressure drop with and without bubbles divided by the pressure drop per unit void fraction $(\Delta p_w/\Delta p_{L0} - 1)/\epsilon$ vs contraction ratio C_R in a vertical nozzle. $\epsilon(0) = 0.1$, $V_t = 25$ cm s^{-1}, $D_n = 3$ cm and $U_L = 52$ cm s^{-1}.

condition removed the change in momentum flux in the liquid and the pressure drop is greater, as noted in figure 18. The agreement between the theory and experiment is now close. However, the main conclusion is that the two-phase pressure correction is quite sensitive to this term depending on the slip/no-slip boundary condition.

It was noted from figure 18 that for small values of void fraction ($\epsilon(0) < 0.1$) the variation in the graphs is linear. In figure 19 we plot the initial gradient of the normalized pressure drop in figure 17 $\{[(\Delta p_w/\Delta p_{L0}) - 1]/0.1\}$ vs the contraction ratio C_R of the nozzle, for a value $u_L/V_t \approx O(1)$, and with the no-slip condition imposed on the bubbles. It is seen that the gradient increases with C_R as expected, but as C_R increases further the gradient asymptotes to a constant value. We do not know at this stage if this behaviour is present over a greater range of liquid velocities.

6. CONCLUSIONS

A one-dimensional gas–liquid flow model has been developed to describe the motion of a bubble in an accelerating flow. The presence of a dilute void fraction of bubbles has also been accounted for in the mass conservation equation for the total liquid flow. This theoretically derived equation is equivalent to the empirical Zuber & Findlay (1965) relation for straight pipes, and low void fraction.

The analytical model has been applied to the particular case of bubbly flow in a linear nozzle and the variation of bubble velocity, liquid velocity, gas void fraction and the liquid pressure terms have been analysed. It has been shown that the bubbles are accelerated and the relative velocity between the bubbles and the liquid increases on passing through the nozzle. Thereafter the bubbles are acted upon by drag. This mechanism affects the behaviour of void fraction through the nozzle which is shown to be sensitive to the variation of relative velocity with bubble velocity. An interesting prediction of the model is that the void fraction is unchanged on passing through a horizontal nozzle. The results have been compared, where possible, to relevant available experimental data. The analysis predicts an increase in mean void fraction through the nozzle which is consistent with the measurements of Thang & Davis (1979) and good agreement exists between the measurements and the predictions for pressure drop in a converging nozzle.

There remain some fundamental questions about the appropriate boundary condition of the velocity on the bubble and about the definition of the pressure field measured at the wall.

Acknowledgements—The authors are grateful for helpful conversations with G. K. Batchelor and M. Escudier. R. Kowe would like to thank Schlumberger Cambridge Research for the financial support received during this work.

REFERENCES

AUTON, T. R. 1987 The lift force on a spherical body in a rotational flow. *J. Fluid Mech.* **183,** 199–218.

AUTON, T. R., HUNT, J. C. R. & PRUD'HOMME, M. 1988 On the motion of cylinders and spheres in inviscid unsteady, non-uniform rotational flows. *J. Fluid Mech.* In press.

BATCHELOR, G. K. 1967 *An Introduction to Fluid Mechanics.* Cambridge Univ. Press, Cambs.

BROOKE-BENJAMIN, T. 1986 Note on added mass and drift. *J. Fluid Mech.* **169,** 251–256.

CLIFT, R., GRACE, J. R. & WEBER, M. E. 1978 *Bubbles, Drops and Particles.* Academic Press, London.

COOK, T. L. & HARLOW, F. H. 1984 Virtual mass in multiphase flow. *Int. J. Multiphase Flow* **10,** 691–696.

COULSON, J. M., RICHARDSON, J. F., BACKHURST, J. R. & HARKER, J. H. 1978 *Chemical Engineering,* Vol. II 3rd edn. Pergamon Press, Oxford.

DARWIN, C. 1953 Note on hydrodynamics. *Proc. Camb. phil. Soc.* **49,** 342–354.

DREW, D., CHENG, L. & LAHEY, R. J. JR 1979 The analysis of virtual mass effects in two-phase flow. *Int. J. Multiphase Flow* **5,** 233–242.

GOVIER, G. W. & AZIZ, K. 1982 *The Flow of Complex Mixtures in Pipes.* Krieger, New York.

HINZE, J. O. 1962 Momentum and mechanical energy balance equations for a flowing homogeneous suspension with slip between the two phases. *Appl. scient. Res.* **A11,** 33–46.

LAMB, H. 1932 *Hydrodynamics.* Cambridge Univ. Press, Cambs.

LANCE, M. 1986 Etude de la turbulence dans les ecoulements disphasiques disperses. Ph.D. Dissertation, Université Claude Bernard, Lyon, France.

LEWIS, D. A. & DAVIDSON, J. F. 1985 Pressure drop for bubbly gas–liquid flow through orifice plates and nozzles. *Chem. Engng Res. Des.* **63,** 149–156.

MILNE-THOMSON, L. M. 1968 *Theoretical Hydrodynamics.* Macmillan, London.

NOORDZIJ, L. 1973 Shock waves in mixtures of liquids and air bubbles. Ph.D. Dissertation, Technological University Twente, Enschede, The Netherlands.

PROSPERETTI, A. & JONES, A. V. 1984 Pressure forces in disperse two-phase flow. *Int. J. Multiphase Flow* **10,** 425–440.

SPALDING, D. B. 1980 Mathematical methods in nuclear reactor thermal hydraulics. Keynote Address at *ANS Mtg on Nuclear Reactor Thermal Hydraulics*, Saratoga, N.Y.

SPEDDING, P. L., CHEN, J. J. J. & NGUYEN, V. T. 1982 Pressure drop in two phase gas–liquid flow in inclined pipes. *Int. J. Multiphase Flow* **8,** 407–431.

THANG, N. T. & DAVIS, M. R. 1979 The structure of bubbly flow through venturis. *Int. J. Multiphase Flow* **5,** 17–37.

THOMAS, N. H., AUTON, T. R., SENE, K. & HUNT, J. C. R. 1983 Entrapment and transport of bubbles by transient large eddies in multiphase turbulent shear flow. Presented at *Int. Conf. on the Physical Modelling of Multiphase Flow*, Coventry, W. Midlands, Paper E1.

VAN WIJNGAARDEN, L. 1976 Hydrodynamic interaction between gas bubbles in liquid. *J. Fluid Mech.* **77,** 27–44.

WALLIS, G. B. 1969 *One Dimensional Two Phase Flow.* McGraw-Hill, New York.

ZUBER, N. & FINDLAY, J. A. 1965 Average volumetric concentration in two-phase flow systems. *J. Heat Transfer Trans. ASME Ser. C* **87,** 453–468.

APPENDIX A

The Drag Force

The drag force caused by the pressure distribution around the bubble being changed by the viscous stresses in the flow around the bubble is a function of the radius a, the density of the liquid and the relative velocity $(v_i - u_{0i})$. It is also a function of the non-uniform and unsteady flow around the bubble, but these effects are ignored here. The usual dimensional scaling, using a drag coefficient C_D, leads to

$$F_{Di} = -0.5\rho_L C_D(v_i - u_{0i})|v_i - u_{0i}|\pi a^2, \qquad [A.1]$$

where C_D is an empirically known function of the Reynolds number of the relative velocity,

$$\mathrm{Re} = \frac{|v_i - u_{0i}|a}{\nu}; \qquad [A.2]$$

see Clift *et al.* (1978).

In many situations it is more convenient to express F_D in terms of the observed value of the rise velocity V_t rather than the unknown drag coefficient and the bubble radius, using the relation

$$0.5\rho_L C_D \pi a^2 V_t^2 = |\Delta\rho| gV.$$

Then [A.1] becomes

$$F_{Di} = -\rho_L \frac{|\Delta\rho|}{\rho_L} Vg \frac{(v_i - u_{0i})|v_i - u_{0i}|}{V_t^{*2}}, \qquad [A.3]$$

where V_t^* is that value of the rise velocity in still liquid for the same value of C_D as for the bubble in the moving liquid. For a pure liquid, whether at high or low Reynolds number, $C_D \propto 1/\mathrm{Re}$. This

leads to

$$F_{Di} = -\rho_L \frac{|\Delta\rho|}{\rho_L} Vg \frac{(v_i - u_{0i})}{V_t}, \quad [A.4]$$

where V_t is the *actual* rise velocity of that particular bubble.

For a bubble in dirty water at high Reynolds number where C_D is approximately constant,

$$F_{Di} = -\rho_L \frac{|\Delta\rho|}{\rho_L} Vg \frac{(v_i - u_{0i})|v_i - u_{0i}|}{V_t^2}, \quad [A.5]$$

where V_t is the actual rise velocity.

To cover the most common situations [A.4] and [A.5], we write

$$F_{Di} = -\rho_L \frac{|\Delta\rho|}{\rho_L} Vg \frac{(v_i - u_{0i})}{V_t} f\left(\frac{|v_i - u_{0i}|}{V_t}\right). \quad [A.6]$$

where $f = 1$ or $f = |v_i - u_{0i}|/V_t$. This form is *not* as general as writing F_D in the form of [A.1] or [A.3]. But other uncertainties are probably more serious.

APPENDIX B

In this section we summarize the equations derived in the preceding sections for a single gas bubble in an accelerating flow. The symbols are defined in sections 1 and 2.

The interfacial force acting on a single bubble with the average volume V is given by

$$F_i = \rho_L V \left\{(1 + C_m)\frac{Du_{0i}}{Dt} - C_m \frac{dv_i}{dt} - g_i - [C_L(v - u_0) \times \omega]_i\right\} + F_{Di}. \quad [B.1]$$

The mass conservation equations for the bubbles in three-dimensional flow are as follows:

$$\frac{\partial}{\partial x_i}[u_{0i}(1 - \epsilon) + C_m \epsilon(v_i - u_{0i})] = 0, \quad [B.2]$$

for the liquid; and

$$\frac{\partial}{\partial x_i}(\epsilon v_i) = 0, \quad [B.3]$$

for the gas phase.

The relations between the different average pressure fields and the flow in a duct are given by

$$\langle p \rangle = p_0 - \frac{0.5\epsilon}{(1 - \epsilon)} C_m (v - u_0)^2, \quad [B.4]$$

where $\langle p \rangle \approx p_w$, and p_0 satisfies the equation

$$\frac{d}{dx_1}[A(p_0 + \rho_L u_{01}^2 + \delta M_1)]$$

$$= p_w \frac{dA}{dx} - A\left\{\epsilon\left[\frac{\bar{F}_1}{V} + \rho_L C_m\left(\overline{\frac{\partial v_1}{\partial t}} - \frac{\partial u_{01}}{\partial t}\right) - \rho_L v_1 \frac{\partial u_{01}}{\partial x_1}\right] + \rho_L(1 - \epsilon)\left(\frac{\partial u_{01}}{\partial t} - g_1\right)\right\} dV, \quad [B.5]$$

where

$$\delta M_1 = \tfrac{1}{2} C_m \rho_L \overline{(v_1 - u_{01})^2}(\lambda - 1)\frac{\epsilon}{(1 - \epsilon)}. \quad [B.6]$$

Equations [B.1]–[B.6] are complete and can provide solutions for all the variables.

APPENDIX C

It is required to solve the differential equation [28] together with the mass conservation equations [B.2] and [B.3]. For a dilute concentration of bubbles ($\epsilon \leqslant 0.1$) we consider the interstitial liquid

velocity u_0 and the bubble velocity v to be perturbed from their respective values $u_o^{(0)}$ and $v^{(0)}$ in a flow containing a single bubble, due to the presence of a void fraction $\epsilon(0)$ of bubbles, where (0) denotes the conditions at the start of the contraction ($x = 0$). Writing

$$u_0 = u_0^{(0)} + \epsilon(0)u',$$
$$v = v^{(0)} + \epsilon(0)v', \qquad [C.1]$$

where $'$ denotes first-order perturbation terms, Equation [25] implies

$$C_m[v^{(0)} + \epsilon(0)v']\frac{d}{dx}[v^{(0)} + \epsilon(0)v'] = (1 + C_m)[u_0^{(0)} + \epsilon(0)u'] \times \frac{d}{dx}[u_0^{(0)} + \epsilon(0)u']$$
$$+ g\cos\alpha - \frac{g}{V_t}[v^{(0)} - u_0^{(0)} + \epsilon(0)(v' - u')]. \qquad [C.2]$$

Equations [4] and [7] give

$$u_{LS}A = u_{LS}(0)A(0) = \{(1 - \epsilon)[u_0^{(0)} + \epsilon(0)u'] + C_m\epsilon[v^{(0)} - u_0^{(0)} + \epsilon(0)(v' - u')]\}A \qquad [C.3]$$

and

$$\epsilon[v^{(0)} + \epsilon(0)v']A = \epsilon(0)[v^{(0)}(0) + \epsilon(0)v'(0)]A(0). \qquad [C.4]$$

Comparing zero-order terms in [C.2] and [C.3],

$$C_m v^{(0)}\frac{dv^{(0)}}{dx} = (1 + C_m)u_0^{(0)}\frac{du_0^{(0)}}{dx} - \frac{g}{V_t}(v^{(0)} - u_0^{(0)}) + g\cos\alpha \qquad [C.5]$$

and

$$u_0^{(0)}A = u_0^{(0)}(0)A(0). \qquad [C.6]$$

Equation [C.5] is the equation of motion of a single bubble in the nozzle. Equation [C.6] states that for a small bubble whose volume can be ignored, as a first approximation, the liquid flow rate through the nozzle is constant.

Comparison of the first-order terms in [C.2]–[C.4] implies

$$v^{(0)}\frac{dv'}{dx} + v'\frac{dv^{(0)}}{dx} = (1 + C_m)\left(u_0^{(0)}\frac{du'}{dx} + u'\frac{du_0^{(0)}}{dx}\right) - \frac{g}{V_t}(v' - u'), \qquad [C.7]$$

$$u' = \frac{\epsilon}{\epsilon(0)}[(1 + C_m)u_0^{(0)} - v^{(0)}] \qquad [C.8]$$

and

$$\epsilon v^{(0)}A = \epsilon(0)v^{(0)}(0)A(0). \qquad [C.9]$$

Equations [C.5]–[C.9] and [B.5] are solved by numerical integration for $u_0^{(0)}$, $v^{(0)}$, ϵ, u', v' and the pressure terms in that order, for different initial values of liquid velocity, void fraction and different angles of inclination of the nozzle whose physical dimensions are specified.

APPENDIX D

To derive the result in [22] we consider the case of a bubble radius a, volume V moving with velocity v parallel to the liquid which has a velocity u_0 (see figure D1). The velocity potential ϕ

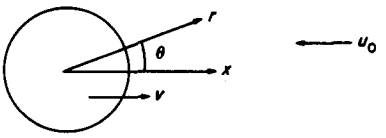

Figure D1. Definition sketch of a stationary bubble in a uniform velocity for calculation of λ in appendix D.

for such a flow (Batchelor 1967, p. 452), in spherical polar coordinates moving with the bubble ($\theta = 0$ corresponds to the direction of motion), is

$$\phi = U_0 x + \tfrac{1}{2} U_0 a^3 \frac{x}{r^3}, \qquad [D.1]$$

where $U_0 = (v - u_0)$, and

$$\frac{\partial \phi}{\partial x} = U_0 + \tfrac{1}{2} U_0 \frac{a^3}{r^3} - \tfrac{3}{2} U_0 a^3 \frac{x^2}{r^5} = U_0 + \tfrac{1}{2} U_0 \frac{a^3}{r^3}(1 - 3\cos^2\theta). \qquad [D.2]$$

The difference in velocity between the liquid near the bubbles and the unperturbed liquid is then

$$\tfrac{4}{3}\pi a^3(\langle u_1^2 \rangle - u_{01}^2) = \int_a^\infty \left[\left(\frac{\partial \phi}{\partial x}\right)^2 - \left(\frac{\partial \phi}{\partial x}\right)_0^2 \right] \mathrm{d}V$$

$$= \int_0^\infty \int_0^\pi \left[u_0^2 \frac{a^3}{r^3}(1 - 3\cos^2\theta) + \tfrac{1}{4} U_0^2 \frac{a^6}{r^6}(1 - 3\cos^2\theta)^2 \right] 2\pi r^2 \sin\theta \, \mathrm{d}r \, \mathrm{d}\theta. \qquad [D.3]$$

Integrating over θ eliminates the first integral. Thence the integral gives

$$\langle u_1 \rangle^2 - u_{0_1}^2 = \tfrac{1}{5} U_0^2 = \frac{\lambda}{2} C_m U_0^2,$$

where

$$C_m = \tfrac{1}{2} \quad \text{and} \quad \lambda = \tfrac{4}{5}. \qquad [D.4]$$